LAWRENCE
LIVERMORE
NATIONAL
LABORATORY

UCRL-PROC-220628

Deformation of nanocrystalline materials at ultrahigh strain rates

Y.M. Wang, E.M. Bringa, M. Victoria, A. Caro,
J.M. McNaney, R. Smith, B.A. Remington

April 18, 2006

8th International Conference on Mechanical and Physical Behavior of Materials Under Dynamic Loading (Dymat 2006)
Dijon, France
September 11, 2006 through September 15, 2006

Disclaimer

This does was performed under the auspices of the U.S. Department of Energy by the University of California, Lawrence Livermore National Laboratory under Contract No. W-7405-Eng-48.

Deformation of nanocrystalline materials at ultrahigh strain rates — microstructure perspective in nanocrystalline nickel

Y. M. Wang*, E.M. Bringa, M. Victoria, A. Caro, J.M. McNaney, R. Smith, and B.A. Remington

Lawrence Livermore National Laboratory, Livermore, CA 94550, USA

Abstract: Nanocrystalline materials with grain sizes smaller than 100 nm have attracted extensive research in the past decade. Due to their high strength, these materials are good candidates for high pressure shock loading experiments. In this paper, we investigated the microstructural evolutions of nanocrystalline nickel with grain sizes of 10-50 nm, shock-loaded in a range of pressures (20-70 GPa). A laser-driven isentropic compression process was applied to achieve high shock-pressures in a timescale of nanoseconds and thus the high-strain-rate deformation of nanocrystalline nickel. Postmortem transmission electron microscopy (TEM) examinations reveal that the nanocrystalline structures survive the shock deformation and that dislocation activity is the prevalent deformation mechanism when the grain sizes are larger than 30 nm, without any twinning activity at twice the stress threshold for twin formation in micrometer-sized polycrystals. However, deformation twinning becomes an important deformation mode for 10-20 nm grain-sized samples.

1. INTRODUCTION

Nanocrystalline materials are defined as metals and alloys with grain sizes smaller than 100 nm. According to the well-known Hall-Petch relationship [1], the yield stress of the polycrystalline materials σ_y follows

$$\sigma_y = \sigma_0 + k_y d^{-1/2} \qquad (1)$$

where σ_0 is the friction stress for dislocation motion, K_y is the dislocation locking term arising from grain boundaries, and d is the grain size. Due to the small grain sizes, nanocrystalline materials have much higher yield strengths than their coarse-grained counterparts. For example, nanocrystalline nickel with an average grain size of 30 nm has a yield stress of 840 MPa [2], which is at least one order of magnitude higher than the microsized nickel (σ_y~58 MPa [3]). This trait makes nanocrystalline materials very attractive for structural applications.

Because of the high strength, the deformation behavior of these nanocrystalline materials has been extensively investigated over the last decade, using a variety of experimental techniques and molecular dynamics (MD) simulations [4]. Unlike the real-world experimental conditions, however, these MD simulations are ubiquitously carried out at high load and extreme strain rates ($> 10^7$ s^{-1}) in order to achieve a meaningful strain in near picosecond MD time scale. Because of this reason, direct comparisons of experiment results and simulations in nanocrystalline materials become problematic. Experimentally, such high-strain-rate deformation can now be achieved through laser-shock loading at high pressures, and has recently been applied to nanocrystalline materials reported in one of our previous publications [5]. To our knowledge, this is the first time that such high pressure shock experiments have been applied to achieve

* Corresponding author email address: ymwang@llnl.gov

high-strain-rate deformation of nanocrystalline materials and provide a meaningful comparison between experiments and simulations.

In this correspondence, we will focus our attention on microstructural evolution details of nanocrystalline nickel after shock loading at different pressures. In order to investigate the grain size effect on deformation behavior, we have further expanded our experiments into much small grain size regime (<10 nm), where dislocations are believed to be non-operative under normal experimental conditions. In this grain size regime, there is no current experimental data available from shock loading experiments.

2. EXPERIMENTAL

Nanocrystalline nickel used in the shock-loading experiments was prepared by pulsed electrodeposition. The success of such technique to fabricate nanocrystalline materials has been addressed at length in several previous publications [6-8]. The electrodeposition process generally produces thin foils with a thickness of tens of micrometers. This thickness, however, is not sufficient for shock loading experiments due to laser blazing and formation of shock craters. Therefore we custom-electroplated nanocrystalline nickel with a thickness of 300 μm onto the copper substrate. The grain sizes of nanocrystalline nickel were controlled by deposition processing parameters (such as voltage and current). In addition, W was added into nickel electrolyte in order to reduce the grain sizes further down to ~10 nm [6].

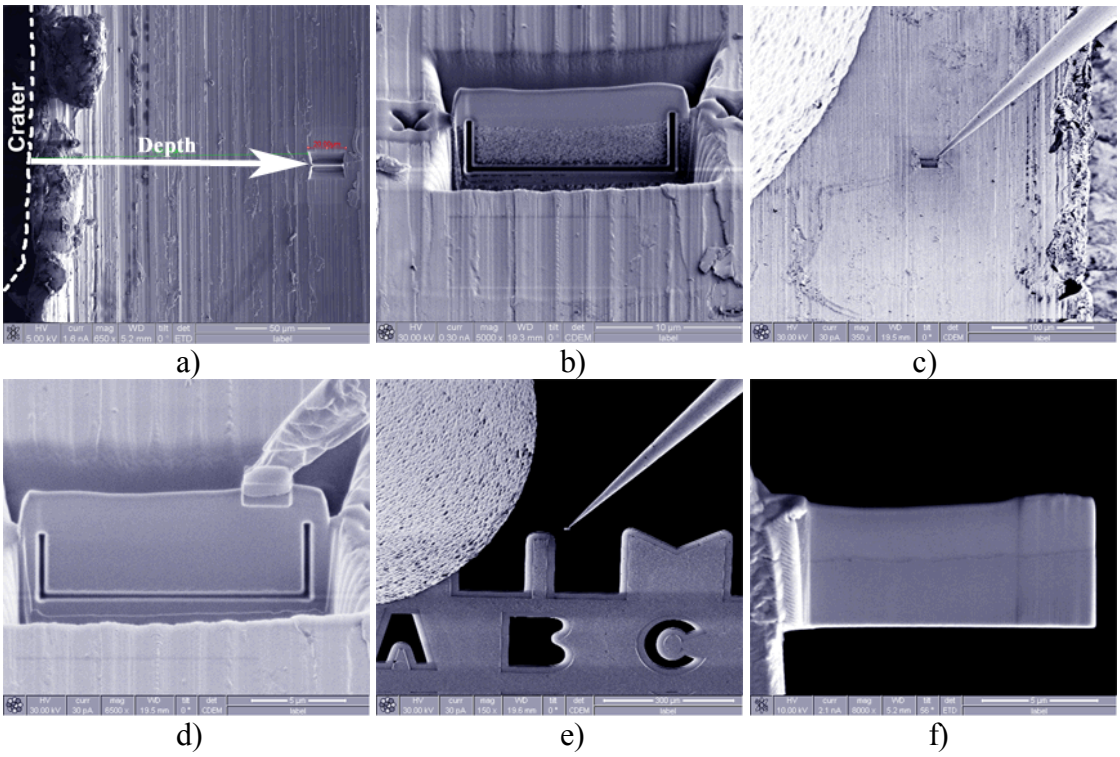

Figure 1. Sequential (a-f) scanning electron microscopy (SEM) images showing focused-ion-beam technique we adopted to prepare cross-sectional TEM samples. (a) The depth from which the TEM sample was lift out is measured by SEM. (b) Focused-ion-beam truncates away the nickel material and leaves a thin slice behind. (c) The lift-out needle approaches the thin slice of Ni. (d) The needle was welded to the thin slice using platinum. (e) The Ni thin slice is transferred to a TEM grid. (f) The thin slice is further thinned by ion-beam and ready for TEM observations.

After electrodeposition, 3 mm diameter cylinders were cut with nanocrystalline nickel on top of the copper substrate for shock loading experiments. Microstructural observations (grain sizes, dislocations, stacking faults, twins, etc.) were performed by transmission electron microscopy (TEM), on both normal plane and a cross-sectional plane of the as-deposited and post-shocked samples, using a Philips CM-300 FEG microscope operated at 300 kV. The shock loading experiments were carried out using high-power

lasers at the Omega and Janus Laser facilities in Rochester, NY and Livermore, CA, respectively. Since nanocrystalline materials are sensitive to the residual heating which could readily lead to rapid grain growth, we have recently developed an isentropic compression driven process to minimize such residual heating effect. This technique also allows us to use sub-millimeter thick samples [9], which is rather significant as the thickness of most nanocrystalline samples is at most several hundred micrometers.

Note that in shock loading experiments, the shock pressure decays slowly along the thickness of the samples. We therefore adopted the focused-ion-beam (FIB) technique (using FEI NOVA 600 Dual-Beam FIB) to prepare TEM samples for microstructural examinations. As shown in Figure 1 (a-f), FIB allowed us to precisely locate the crater position and measure the depth where the TEM samples were lift out. This technique permits us to establish one-on-one correspondence between the observed microstructures and the shock pressures. Since ion beam could induce artifacts into materials during sample preparations, we used electropolishing technique to prepare TEM samples for comparison. In all the cases, we did not discover significant microstructural discrepancies between these two batches of samples.

3. RESULTS

Figure 2 shows the cross-sectional transmission electron microscopy (TEM) images of nanocrystalline nickel with an average grain size of 40 nm and 15 nm, respectively. In order to electroplate the smaller grain sizes (Figure 2b) [6], a 13 wt.% tungsten content was added during the electrodeposition. Extensive TEM examinations indicate that W forms complete solid solution with nanocrystalline nickel without any sign of precipitates (see Figure 2b). The grain sizes along the cross-section are slightly elongated but relatively uniform.

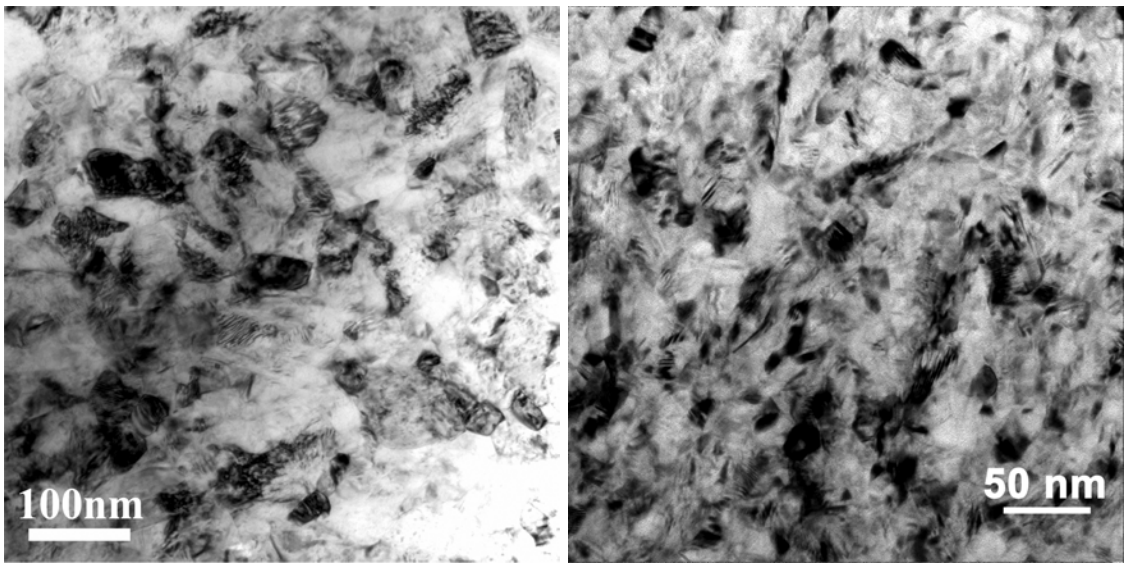

Figure 2. Cross-sectional transmission electron microscopy images of nanocrystalline nickel with an average grain size of (a) 40 nm, and (b) 15 nm. Slightly elongated grain structures are observed along the cross-section due to columnar grain growth nature of the electrodeposited materials. The average grain size was determined by measuring the sizes of over 200 individual nanograins from a number of TEM images such as the ones shown above.

Despite the use of copper substrate, powerful laser shock created a crater at the place where the loading was applied, as shown in Figure 3. The size of such a crater is roughly equal to the size of the laser spot (~1mm^2), and the depth is 20-100 μm, depending on the shock pressures. It was observed that the craters generated in nanocrystalline nickel were much shallower than those seen in coarse-grained polycrystalline nickel due to the higher yield strength of the nanocrystalline materials. Near the center of the spot, the shock loading is very close to uniaxial and produces strains of 8% and 13% at shock pressures of 20 GPa and 40 GPa, respectively, as predicted by Hugoniot data.

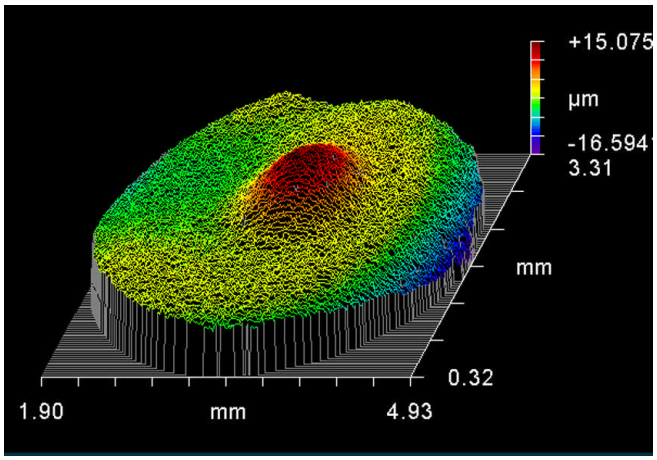

Figure 3. An Ambios white light profilometry image of the nanocrystalline nickel after shock loading, showing the backside of a crater generated by the laser shock.

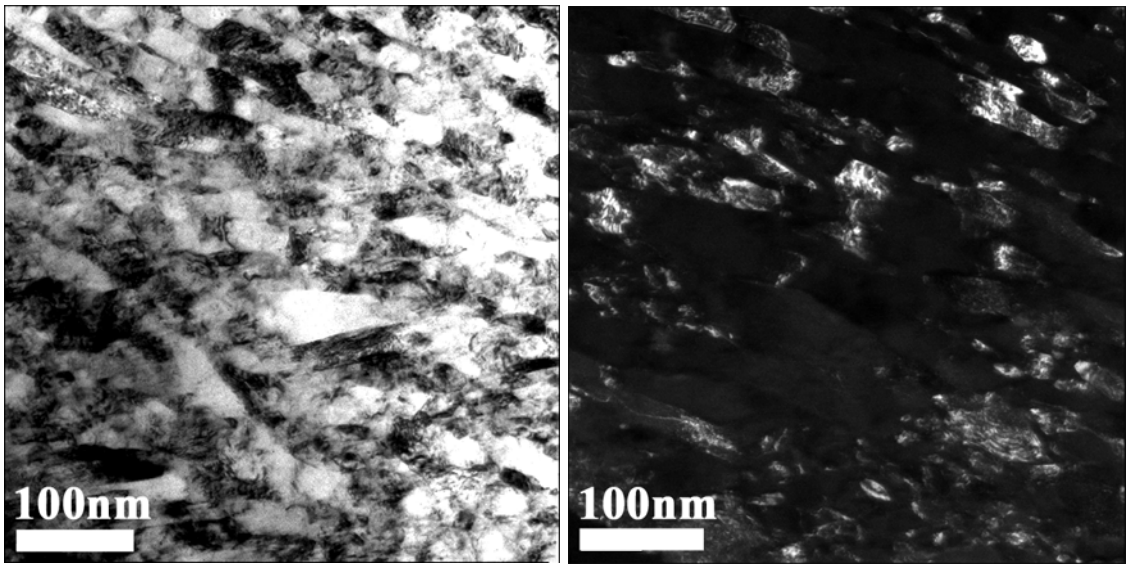

Figure 4. Cross-sectional (a) Bright- and (b) dark-field (DF) TEM images of nanocrystalline Ni after shock loading at the pressure of 40 GPa. High density of dislocations is observable, which can be better resolved in the DF image. The dislocation density was estimated to be as high as ~10^{16} /m^2.

All the microstructures reported in this paper were obtained underneath the center of the craters. For each shock pressure, TEM samples were prepared by taking the thin slices from the depth of 50 μm, 100 μm, and 150 μm respectively below the crater surface. Except at the very surface of the samples (<50 μm), similar microstructures were observed underneath the craters when the depth is greater than 100 μm. Shown in Figure 4 are cross-sectional TEM images of nanocrystalline nickel with grain sizes of 30-50 nm shock-loaded at 40 GPa and at the depth of 150 μm. It can be clearly seen from these images that nanocrystalline structures survive shock loading. Minor grain growth was observed after careful TEM examinations of the samples taken from different depths. Dislocation debris is visible in the bright-field image (Figure 4a), but is better resolved in the dark-field (Figure 4b). The density of dislocations is measured to be as high as 10^{16} /m^2 at this shock pressure. Such high dislocation density in nanocrystalline materials is quite unusual and cannot be induced through normal deformation conditions [5]. We have also

examined the microstructures of the same nanocrystalline nickel (30-50 nm) after shock loading at the pressures of 20 GPa and 65 GPa. In all the cases, dislocations are the predominant deformation debris, suggesting that the plastic deformation of 30-50 nm grain-sized nickel under shock loading is likely accommodated by dislocation generations and movements. This is in stark contrast with the results seen in coarse-grained nickel, where deformation twinning becomes the important mode of deformation at the shock pressure of 30 GPa [10-12]. Within the shock pressure (up to 65 GPa) investigated, stacking faults and/or deformation twins were never observed for the nanocrystalline nickel with grain sizes of 30-50 nm.

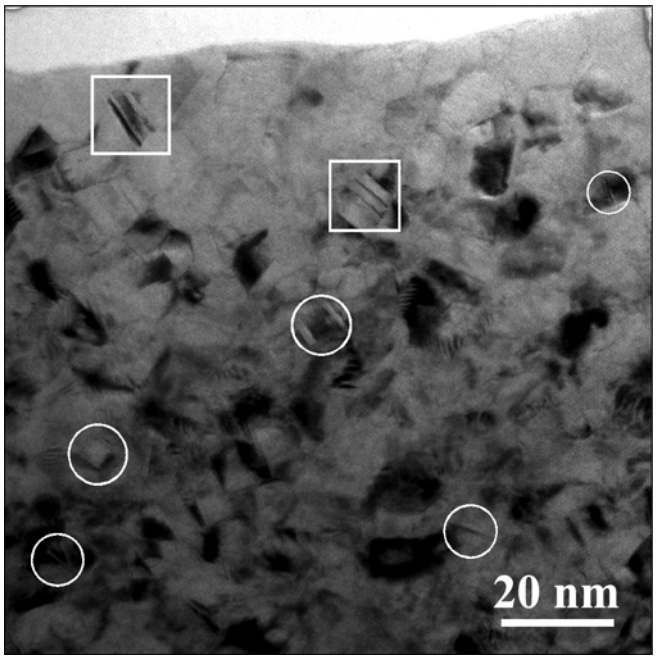

Figure 5. Cross-sectional TEM micrograph of nanocrystalline Ni-W sample after shock loading at 38 GPa. The twins are accentuated in the white squares and circles.

In order to understand the grain size effect on deformation behavior, we also studied the microstructures of nanocrystalline Ni with grain sizes of 10-15 nm after shock loading at 38 GPa. In contrast to the high-density of dislocations seen in the above-mentioned samples, deformation twins are the principal defect structures observed in these samples. The morphology of these deformation twins is not very different from the conventionally formed ones (they resemble arrays of stacking faults), except that the twinning lamellae are much narrow within the nanograins, as shown in Figure 5. The as-deposited nanocrystalline Ni samples have a very low density of pre-existing growth twins, which usually appear in bundles with multiple lamellae parallel to each other (such as those highlighted with white square in Figure 5). After shock-loading, the twin density is observed to increase drastically, suggesting that deformation twinning becomes an important event during shock loading of this smaller grain-size nickel.

The observation of deformation twinning in nanocrystalline Ni is an interesting phenomenon in several respects. First, recent MD simulations [13] proposed that the tendency of full/partial dislocation or twinning mechanism in nanocrystalline materials is determined by the ratio of the unstable to the stable stacking fault energies. This quantity is 0.55 for Ni (in comparison to Al, 0.97; Cu, 0.13), suggesting that twinning is a difficult event in nanocrystalline Ni and thus has rarely been documented [14]. Our experimental results support such hypothesis and demonstrate that twinning possibly occurs at very high deviatoric stresses in nanocrystalline Ni. Second, the grain-size dependence of twinning stress in the literature is a matter of controversy. Many dislocation-based models have predicted that [15], at a certain pressure, large grain-sized materials twin more readily than small grain-sized ones. This is unlikely the case here. As the grain size decreases down to 10-15 nm, twinning becomes the preferred mode of plastic deformation. Third, the observed twinning activity in the small grain-sized samples (10-15 nm) is consistent with our recent molecular dynamics (MD) simulations of shocked nanocrystalline samples [16], where partial dislocations/stacking faults dictate plastic deformation at grain sizes below 15 nm. At larger

grain sizes, on the other hand, our MD simulations show a large number of full dislocations [16]. The dislocation density in MD simulations is about one order of magnitude higher than the one estimated from the TEM investigations. This is probably attributed to the fact that a large number of dislocations disappeared during the recovery process (due to small thermal heating and stress unloading). The deformation twinning is negligible in MD simulations for 20-40 GPa shock pressure when the grain sizes are larger than 30 nm. Finally, it is noteworthy pointing out that the deformation twinning observed in 10-20 nm nickel during shock loading could also be attributed to the reduced stacking fault energy in nanocrystalline Ni because of the addition of tungsten. Extensive computational effort is currently ongoing in our group to elucidate the stacking fault energy effect on deformation twinning behavior of nanocrystalline materials.

4. SUMMARY

We have investigated the deformation behavior of nanocrystalline nickel with grain sizes of 10-50 nm under different shock pressures. The experimental evidence acquired through postmortem transmission electron microscopy examinations suggests that the dislocation mechanism remains an important mode of deformation when the grain size of nanocrystalline Ni is still large (>30 nm) and the shock pressure is below 70 GPa. In contrast, deformation twinning becomes an important event as the grain size decreases below 10-20 nm, suggestive of grain-size dependent deformation mechanisms in nanocrystalline materials under shock loading conditions.

Acknowledgements

The authors wish to thank Prof. C.A. Schuh and Mr. A. Detor (both at MIT) for providing nanocrystalline nickel samples, Mrs. Laura Cook and Mr. Nick Teslich for their assistance on hardness measurements and TEM sample preparations, respectively.

References

1. J. R. Weertman, in Nanostructured materials, edited by C.C. Koch (Norwich, NY, Noyes Publications, 2002).
2. Y.M. Wang, S. Cheng, Q.M. Wei, E. Ma, T.G. Nieh, and A.V. Hamza, *Scr. Mater.* **51** (2004) 1023-1028.
3. Y.M. Wang and E. Ma, *Appl. Phys. Lett.* **85** (2004) 2750-2752.
4. V. Yamakov, D. Wolf, S.R. Phillpot, A.K. Mukherjee, and H. Gleiter, *Phil. Mag. Lett.* **83** (2003) 385-390.
5. Y.M. Wang, E.M. Bringa, J.M. McNaney, M. Victoria, A. Caro, A.M. Hodge, R. Smith, B. Torralva, B.A. Remington, C.A. Schuh, H. Jamarkani, and M.A. Meyers, *Appl. Phys. Lett.* **88** (2006) 061917.
6. T. Yamasaki, *Scr. Mater.* **44** (2001) 1497-1503.
7. G. D. Hibbard, J. L. McCrea, G. Palumbo, K. T. Aust, and U. Erb, *Scr. Mater.* **47** (2002) 83-87.
8. F. Jankowski, C.K. Saw, J.F. Harper, B.F. Vallier, J.L. Ferreira, and J.P. Hayes, *Thin Solid Films* **494** (2006) 268-273.
9. J. Edwards, K.T. Lorenz, B.A. Remington, S. Pollaine, J. Colvin, D. Braun, B.F. Lasinski, D. Reisman, J.M. McNaney, J.A. Greenough, R. Wallace, H. Louis, and D. Kalantar, *Phys. Rev. Lett.* **92** (2004), 075002.
10. E.V. Esquivel, L.E. Murr, E.A. Trillo, and M. Baquera, J. Mater. Sci. **38** (2003) 2223-2231.
11. P.S. Follansbee and G.T. Gray, Int. J. Plasticity **7** (1991) 651-660.
12. F. Greulich and L.E. Murr, Mater. Sci. Eng. **39** (1979) 81-83.
13. H. Van Swygenhoven, P.M. Derlet, and A.G. Frøseth, Nat. Mater. **3** (2004) 399-403.
14. X. L. Wu, E. Ma, *Appl. Phys. Lett.* **88** (2006) 061905.
15. M.A. Meyers, O. Vöhringer, and V.A. Lubarda, *Acta Mater.* **49** (2001) 4025-4039.
16. E.M. Bringa, A. Caro, Y.M. Wang, M. Victoria, J.M. McNaney, B.A. Remington, R.F. Smith, B. Torralva, and H. Van Swygenhoven, *Science* **309** (2005) 1838-1841.